

Rapid thermal annealing of MeV erbium implanted LiNbO₃ single crystals for optical doping

M. Fleuster and Ch. Buchal

Institut für Schicht- und Ionentechnik (ISI), Forschungszentrum Jülich, D-52425 Jülich, Germany

E. Snoeks and A. Polman

FOM-Institute for Atomic and Molecular Physics, Kruislaan 407, 1098 SJ Amsterdam, The Netherlands

(Received 7 February 1994; accepted for publication 9 May 1994)

LiNbO₃ single crystals (*x* cut) were implanted with 3.5-MeV Er ions with fluences up to 3×10^{16} cm⁻². Upon annealing the implantation-amorphized surface layer regrows epitaxially, displaying either columnar or planar layer-by-layer growth, depending on the rate at which the samples are brought to the final temperature of 1060 °C. Low heating rates (≈ 10 °C/s) result in columnar regrowth, and 8-h anneals are necessary for complete dissolution of the grain boundaries. In contrast, using a rapid warm-up (100 °C/s), annealing for 1 min at 1060 °C is sufficient to restore a perfect crystal without grain boundaries. The advantage of the short anneal is that it leads to only minimal diffusion broadening of the Er profile. The maximum concentration of optically active Er ions is 0.18 at. %.

The success of the Er-doped optical fiber amplifiers has stimulated activities to use similar concepts in planar integrated optics by incorporating Er into planar waveguide devices. The Er³⁺ ion shows an optical (intra-4*f*) transition around 1.5 μm, a standard telecommunication wavelength. LiNbO₃ is a key material for integrated optics due to its excellent electro-optical and nonlinear optical properties. In an Er:LiNbO₃ waveguide the optical gain produced by the Er ions could be used to compensate for the intrinsic losses of an integrated optical device (e.g., a switch or a modulator). In addition, the electro-optical properties can be used to fabricate advanced laser structures like mode-locked or *Q*-switched waveguide lasers. Recently, the first mode-locked waveguide laser based on Er-doped LiNbO₃ was presented.¹

The Er lasing scheme is a three-level system, and therefore the 1.5-μm signal is absorbed by the Er³⁺ ions in the ground state. Hence the performance of optical waveguide lasers and amplifiers in Er-doped LiNbO₃ depends critically on the shape and the position of the Er depth profile.² Up to now the LiNbO₃ substrates used for the fabrication of active waveguide devices have been doped by indiffusion from the surface.^{3,4} The performance of these devices is still far from the theoretical optimum, since the indiffused Er profile has its maximum at the surface. There, on the other hand, the pump light intensity is close to zero.⁵ Recently, we showed that ion implantation of Er into LiNbO₃ with MeV energies is a very attractive approach since it allows the adjustment of the Er depth distribution on a micrometer depth scale, the typical dimension of optical waveguides.⁵ Furthermore, implantation allows one to raise the Er concentration beyond the equilibrium solubility. We showed that annealing of the Er implanted samples in a tube furnace causes the recrystallization of the amorphized surface layer by columnar solid-phase epitaxial regrowth (SPE).⁶ The resulting grain boundaries do not influence the photoluminescence (PL) of the Er ions but the low crystal quality of the surface layer is unfavorable for waveguiding operation. Annealing for 8 h at

1060 °C is necessary to remove all grain boundaries, leading to significant diffusion broadening of the Er profile.

In this letter we show that the columnar SPE regrowth can be avoided completely by rapidly heating the implanted LiNbO₃ samples to the final annealing temperature. Using a rapid thermal annealer (RTA) at a heating rate of about 100 °C/s, no columns are formed, and an amazingly short annealing time of 1 min at 1060 °C is sufficient to cause perfect epitaxial recrystallization. Using this procedure, a concentration of up to 0.18 at. % optically active Er ions can be incorporated into the LiNbO₃ lattice.

X-cut LiNbO₃ single crystals (Crystal Technology) were implanted at room temperature with Er ions at 3.5 MeV. The implantation fluences ranged from 5×10^{15} to 3×10^{16} ions/cm². Thermal annealing was performed either in a RTA with various heating rates under flowing oxygen or in a quartz tube furnace in a wet oxygen atmosphere to suppress Li outdiffusion.⁷ The samples were put into the preheated furnace, resulting in an initial heating rate of ~ 10 °C/s. Beyond 600 °C, the temperature rise slows down.

The crystal quality after annealing was studied using Rutherford backscattering spectrometry (RBS) and channeling. In addition, samples were analyzed by transmission electron microscopy (TEM). The Er concentration profiles were determined by secondary-ion-mass spectrometry (SIMS), using O⁺ to sputter an area of 150×150 μm². PL spectroscopy was performed at room temperature using the 496.5-nm line of an Ar-ion laser as an excitation source with a power of 100 mW. The signal was analyzed with a 48-cm monochromator and detected by a liquid-nitrogen-cooled Ge detector, yielding a spectral resolution of 3 nm. Time-resolved luminescence decay measurements were carried out using a 1.5-ms, 500-mW pulse with a cutoff time shorter than 150 μs, obtained by mechanical chopping.

Figure 1 shows the ion channeling spectra of three selected LiNbO₃ samples implanted with a fluence of 5×10^{15} Er/cm² at 3.5 MeV and subsequently annealed at 1060 °C. Also shown are the random and channeling spectra of an

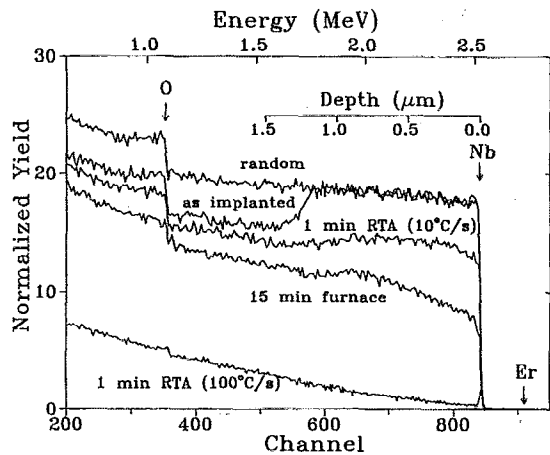


FIG. 1. RBS channeling spectra of Er implanted (3.5 MeV , $5 \times 10^{15} \text{ Er/cm}^2$) LiNbO_3 single crystals (x cut). One sample was annealed for 15 min at 1060°C in a quartz tube furnace (wet oxygen, initial heating rate $\sim 10^\circ\text{C/s}$) while the other samples were annealed for 1 min at 1060°C using the RTA (dry oxygen). The warm-up rates for these anneals are given in brackets. Also shown are random and channeling spectra of the as-implanted sample. The arrows indicate surface channels of the different elements.

as-implanted sample. For this sample the channeling yield in the $1.25\text{-}\mu\text{m}$ -thick surface region is identical to the random yield. TEM shows that this surface layer is indeed fully amorphous.⁶ Annealing one sample in the tube furnace for 15 min at 1060°C results in a reduction of the channeling yield by about a factor of 2. A second sample was annealed for 1 min in the RTA using a rapid heating rate of 100°C/s and shows a significantly different behavior. The minimum yield χ_{min} is only $(2.3 \pm 0.2)\%$, identical to the value of $(2.0 \pm 0.3)\%$ found for virgin crystals. Plan-view TEM confirmed that this sample is a single crystal without any grain boundaries. To exclude that this dramatic difference is a result of a difference in ambient during annealing (wet oxygen in the tube furnace, dry oxygen in the RTA) a third sample was annealed for 1 min at the same temperature in the RTA, using a low heating rate of 10°C/s , comparable to that of the tube furnace. This sample shows a low crystal quality, too (see Fig. 1).

In an earlier publication⁶ we have shown that annealing in the tube furnace causes the amorphous surface region of the as-implanted sample to regrow by a columnar SPE growth mode from the substrate. This occurs already at relatively low temperatures ($\sim 400\text{--}550^\circ\text{C}$) during the slow warming up of the sample to 1060°C . Once formed, these grain boundaries are very stable, and long additional annealing times (8 h) are required to dissolve them. The grain boundaries cause the high channeling yield in the RBS spectra. Such a columnar growth has not yet been described for Ti-implanted LiNbO_3 .^{8,9}

Quite surprisingly, this columnar growth pattern does not occur when the heating rate is high enough. One possible explanation is that at high temperatures (where the crystallization takes place after rapid heating), the formation of defects disturbing the planar growth front is slow relative to the SPE growth rate, whereas it is the other way around at lower temperatures. Such defects may be a result of bulk nucle-

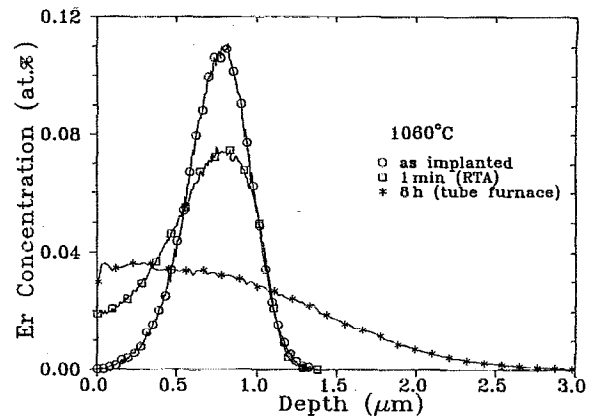


FIG. 2. SIMS depth profiles of Er implanted (3.5 MeV , $5 \times 10^{15} \text{ Er/cm}^2$) LiNbO_3 single crystals, annealed at 1060°C in the tube furnace (8 h) or the RTA (1 min, warm-up rate 100°C/s).

ation in the amorphous layer ahead of the interface (e.g., misoriented crystal LiNbO_3 or Er-oxide precipitates), or they may be created at the moving interface itself (e.g., microtwins or stress related defects). Further work to investigate the thermodynamics and kinetics of the SPE of LiNbO_3 in the presence of rare-earth ions is in progress.

Figure 2 shows the Er depth profiles of three LiNbO_3 samples implanted with $5 \times 10^{15} \text{ Er/cm}^2$ at 3.5 MeV . The as-implanted profile is nearly Gaussian shaped, and peaks at a depth of $0.78 \mu\text{m}$. The peak concentration is $0.11 \text{ at. } \%$. Annealing the sample for 8 h at 1060°C in the tube furnace causes a significant widening of the Er depth profile. Er ions have diffused into the bulk and towards the surface. In contrast, the sample annealed for 1 min at 1060°C using the RTA shows a much sharper profile. The surface concentration has increased as compared to the as-implanted profile, but no Er diffusion into the bulk is observed. The different shape of the two Er depth profiles is a result of the different annealing times: using the very short annealing time in the RTA, the Er diffusion into the bulk can be avoided effectively, and only defect enhanced diffusion of Er ions towards the surface during the recrystallization of the amorphous phase remains. Gain calculations for a waveguide amplifier based on a proton-exchanged waveguide predict a reduction of the threshold pump power by a factor of 2 for the narrower Er profile as compared to the profile of a tube furnace annealed sample due to the improved matching to the optical mode.

Room-temperature PL spectra (not shown) for the samples prepared in both ways are indistinguishable and identical to the spectra found for other samples annealed in the tube furnace.⁶ The measured PL intensity and lifetime (2.8 ms) was the same for both samples, proving that the fraction of the optically active Er ions is the same for both annealing procedures.

Using the short annealing in the RTA (1 min 1060°C , 100°C/s) allows one to study PL intensity and lifetime for high Er concentrations. Er fluences in the range from 5×10^{15} to $3 \times 10^{16} \text{ Er/cm}^2$ were used at 3.5 MeV . RBS/channeling experiments (not shown) prove that this annealing treatment

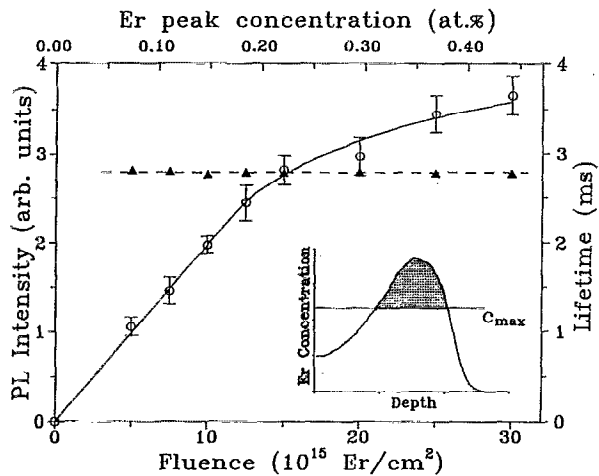


FIG. 3. Photoluminescence intensity (open circles, left axis) and lifetime at 1533 nm (closed triangles, right axis) as a function of the implanted Er fluence. All samples have been implanted with 3.5 MeV and annealed for 1 min at 1060 °C in flowing oxygen using the RTA (warm-up rate 100 °C/s). The Er peak concentration is indicated on the top axis. The dashed line marks the average PL lifetime for all fluences: 2.79 ms. The solid line is a least-mean-square fit, calculated from a model assuming a maximum optically active Er concentration of 0.18 at. %. The inset schematically shows that the fraction of active Er ions decreases below unity if the Er peak concentration exceeds this concentration limit. The shadowed region corresponds to the inactive Er fraction.

causes perfect recovery of the LiNbO_3 lattice up to a fluence of $2.0 \times 10^{16} \text{ Er/cm}^2$. Samples implanted with higher fluences are highly disordered, resulting in a channeling yield close to the random value. The PL spectra of these samples implanted with different fluences have different intensities but nearly identical shapes. Only for the highest fluences (2.5 and $3 \times 10^{16} \text{ Er/cm}^2$) is the width of the PL lines marginally increased, which is explained by inhomogeneous broadening due to the reduced crystal quality as found by RBS. Figure 3 shows the integrated PL intensity as function of the implanted Er fluence. The corresponding Er peak concentration is given on the top axis. Up to a fluence of $1.25 \times 10^{16} \text{ Er/cm}^2$, the PL intensity increases linearly with Er fluence. For higher fluences it levels off. Fluorescence decay measurements at 1533 nm showed a single exponential decay for all samples. The measured lifetime of (2.79 ± 0.05) ms is independent of the implanted Er fluence and is also plotted in Fig. 3.

As the lifetime, hence the fluorescence efficiency, is constant for the whole concentration range, a linear increase of the PL intensity as function of the number of optically active Er ions is expected. The saturation of the PL intensity above $1.25 \times 10^{16} \text{ Er/cm}^2$ suggests that there is a limit to the concentration of optically active Er (c_{max}). The PL intensity would then be proportional to the integrated areal density of Er below c_{max} , which can be calculated for each fluence using the SIMS concentration profile of Fig. 2 scaled with the fluences (see inset of Fig. 3). Indeed, this simple model with $c_{\text{max}} = (0.18 \pm 0.01)$ at. % shows perfect agreement with the data as indicated by the solid line in Fig. 3. Earlier measurements have shown that the equilibrium solubility of Er in LiNbO_3 is 0.125 at. % at 1060 °C.¹⁰ Given the inaccuracy in

temperature calibration for different experiments, c_{max} may be related to the solubility.

There is no indication of energy transfer between adjacent Er ions, and no sign of cooperative upconversion is seen at the employed pump powers. Note that this behavior is totally different from the results found for Er implanted silica glasses:^{11,12} for example, in soda-lime-silicate glass, up to 1 at. % optically active Er ions can be incorporated, but the PL is limited by concentration quenching effects and irradiation-induced defects.¹²

In conclusion, we have demonstrated for the first time perfect epitaxial regrowth of amorphized, Er implanted LiNbO_3 submitted to a single, short (1-min) rapid thermal treatment at 1060 °C using a heating rate of 100 °C/s. In contrast, conventional furnace annealing at a slow heating rate (10 °C/s) leads to a columnar epitaxial growth mode yielding grain boundaries which are only annealed out at 1060 °C for 8 h. The rate dependence is related to differences in the balance between nucleation and growth kinetics at or near to the interface. The short RTA anneals permit the construction of well controlled Er profiles, not significantly affected by diffusion broadening. This is very advantageous for optical device design and fabrication. The optical spectra from Er are identical for both annealing procedures. The maximum concentration for optically active Er ions is 0.18 at. %, and no concentration quenching effects were observed.

We thank H. Holzbrecher from ZCH of KFA Jülich for performing the SIMS measurements and M. Dinand of Universität-GH Paderborn, Germany for providing the gain calculations. We gratefully acknowledge the support from the Tandatron facility and staff at IFF of KFA Jülich. The Dutch part of this work is part of the research program of the Foundation for Fundamental Research on Matter (FOM) and was made possible by financial support from Dutch Organization for the Advancements of Pure Research (NWO), the Netherlands Technology Foundation (STW), and the IC Technology Program (IOP Electro-optics) of the Ministry of Economic Affairs.

- ¹H. Suche, I. Baumann, D. Hiller, and W. Sohler, *Electron. Lett.* **29**, 1111 (1993).
- ²M. Dinand and W. Sohler, *IEEE J. Quantum Electron.* (in press).
- ³R. Brinkmann, W. Sohler, and H. Suche, *Electron. Lett.* **27**, 415 (1991).
- ⁴P. Becker, R. Brinkmann, M. Dinand, W. Sohler, and H. Suche, *Appl. Phys. Lett.* **61**, 1257 (1992).
- ⁵M. Fleuster, Ch. Buchal, H. Holzbrecher, U. Breuer, M. Dinand, H. Suche, R. Brinkmann, and W. Sohler, *Mat. Res. Soc. Symp. Proc.* **279**, 279 (1993).
- ⁶M. Fleuster, Ch. Buchal, E. Snoeks, and A. Polman, *J. Appl. Phys.* **75**, 173 (1994).
- ⁷J. L. Jackel, *J. Opt. Commun.* **3**, 82 (1982).
- ⁸Ch. Buchal, P. R. Ashley, and B. R. Appleton, *J. Mater. Res.* **2**, 222 (1987).
- ⁹D. B. Paker and D. K. Thomas, *J. Mater. Res.* **4**, 412 (1989).
- ¹⁰I. Baumann, R. Brinkmann, Ch. Buchal, M. Dinand, M. Fleuster, H. Holzbrecher, W. Sohler, and H. Suche, in *Proceeding of the European Conference on Integrated Optics (ECIO)*, Neuchâtel, April 1993, pp. 3–14 (unpublished).
- ¹¹A. Polman, D. C. Jacobson, D. J. Eaglesham, R. C. Kistler, and J. M. Poate, *J. Appl. Phys.* **70**, 3778 (1991).
- ¹²E. Snoeks, G. N. van den Hoven, and A. Polman, *J. Appl. Phys.* **73**, 8179 (1993).